Kalman Filtering of Angular-Momentum-Based Attitude Parameters

F. Landis Markley[a] and Joseph E. Sedlak[b]

[a]GN&C Systems Engineering Branch, NASA Goddard Space Flight Center, USA
[b]a.i. solutions, Inc., USA

Abstract

This paper presents an extended Kalman filter using an attitude parameterization that is advantageous for attitude estimation of spinning spacecraft. The parameters are the angular momentum components in an inertial reference frame, the angular momentum components in the body frame, and a rotation angle. To avoid the singularity of the 7×7 covariance of this state vector arising from the constraint that the magnitude of the angular momentum vector is the same in the inertial and body frames, the Kalman filter employs the nonsingular 6×6 covariance of a reduced error state. Three of the components of this six-component error state are the usual infinitesimal attitude error angles, so the usual 3×3 attitude covariance matrix is a submatrix of the 6×6 covariance. The performance of the resulting filter is compared with that of a quaternion-based filter.

Introduction

Attitude estimation is often more difficult for spinning spacecraft than for three-axis stabilized spacecraft. Many conventional state vector elements for representing the spacecraft attitude and its time rate of change vary more rapidly in the spinning case, and gyro rate measurements are often lacking, requiring Euler's equations for modelling the attitude dynamics. This paper employs an angular-momentum-based representation that is advantageous for this application [1]. The seven parameters in this representation are the components of the angular momentum in an inertial reference frame, the angular momentum components in the body frame, and a rotation angle. The parameters are subject to the constraint that the magnitude of the angular momentum vector is the same in the inertial and body frames.

This paper presents a new derivation of this parameterization and develops an extended Kalman filter (EKF) employing it. The constraint causes the covariance of the seven-component state vector to be singular, in parallel with the singularity of the four-component quaternion representation of attitude [2, 3]. To avoid this singularity, the Kalman filter employs the nonsingular 6×6 covariance of a six-component error state. Three of the components of the six-component error state are the usual infinitesimal attitude error angles, so the usual 3×3 attitude covariance matrix is a submatrix of the 6×6 covariance.

This new filter has been fully developed and incorporated into the attitude ground support system used for spinning spacecraft at the NASA Goddard Space Flight Center. A more conventional EKF based on the quaternion and body rotation rate has been developed for comparison. Numerical tests using simulated data patterned after the Space Technology 5 (ST5) spacecraft show that these two filters and the filter reported in [2] have very similar performance.

Angular-momentum-based attitude parameterization

The angular momentum in the spacecraft body frame, $\mathbf{L}_B$, and the angular momentum in an inertial reference frame, $\mathbf{L}_I$, obey the equations of motion [4]

$$\dot{\mathbf{L}}_B = \mathbf{N}_B - \boldsymbol{\omega}_{BI} \times \mathbf{L}_B \quad \text{and} \quad \dot{\mathbf{L}}_I = \mathbf{N}_I = A_{BI}^T \mathbf{N}_B \tag{1ab}$$

as well as the constraint

$$|\mathbf{L}_B| = |\mathbf{L}_I| \equiv L, \tag{2}$$

where A_{BI} is the inertial-to-body attitude matrix. The angular velocity is given by

$$\boldsymbol{\omega}_{BI} = J^{-1}(\mathbf{L}_B - \mathbf{L}_{int}), \tag{3}$$

where the spacecraft moment of inertia tensor and the angular momentum of any moving parts (reaction wheels, steerable antennas or solar arrays, fuel slosh, etc.) relative to the spacecraft are denoted by J and $\mathbf{L}_{int}$, respectively. Spacecraft dynamics is commonly modelled by (1a) and kinematics by

$$\dot{A}_{BI} = -[\boldsymbol{\omega}_{BI}\times] A_{BI}, \tag{4}$$

where

$$[\mathbf{v}\times] \equiv \begin{bmatrix} 0 & -v_3 & v_2 \\ v_3 & 0 & -v_1 \\ -v_2 & v_1 & 0 \end{bmatrix} \tag{5}$$

denotes the cross product matrix. A quaternion or some other lower-dimensional representation of A_{BI} is often integrated rather than (4), but this distinction is not important for this paper. An alternative formulation uses (1b) and

$$\mathbf{L}_B = A_{BI} \mathbf{L}_I, \tag{6}$$

in place of (1a). Both of these formulations have the disadvantage for application to spinning spacecraft that many components of the state vector are fast variables.

The formulation in this paper is based on the observation that the attitude matrix, which can be the most general rotation taking the unit vector $\hat{\mathbf{L}}_B \equiv \mathbf{L}_B / L$ to $\hat{\mathbf{L}}_I \equiv \mathbf{L}_I / L$, can be expressed as

$$A_{BI}(\mathbf{x}) = R(\hat{\mathbf{L}}_B, \zeta_B) R_{BI} R(\hat{\mathbf{L}}_I, \zeta_I), \tag{7a}$$

where

$$R(\mathbf{e}, \phi) \equiv (\cos\phi) I_{3\times 3} + (1 - \cos\phi)\mathbf{e}\mathbf{e}^T - \sin\phi[\mathbf{e}\times] \tag{7b}$$

is the matrix representing a rotation by angle ϕ about axis $\mathbf{e}$, and R_{BI} is any specific rotation taking $\hat{\mathbf{L}}_I$ to $\hat{\mathbf{L}}_B$. We choose this to be the minimum rotation

$$R_{BI} = (\hat{\mathbf{L}}_B \cdot \hat{\mathbf{L}}_I) I_{3\times 3} - \hat{\mathbf{L}}_I \hat{\mathbf{L}}_B^T + \hat{\mathbf{L}}_B \hat{\mathbf{L}}_I^T + (1 + \hat{\mathbf{L}}_B \cdot \hat{\mathbf{L}}_I)^{-1} (\hat{\mathbf{L}}_B \times \hat{\mathbf{L}}_I)(\hat{\mathbf{L}}_B \times \hat{\mathbf{L}}_I)^T. \tag{7c}$$

Multiplying (7a) on the left by $R_{BI}R_{BI}^T$ or on the right by $R_{BI}^T R_{BI}$ and using some matrix identities gives

$$A_{BI}(\mathbf{x}) = R_{BI}R(\hat{\mathbf{L}}_I,\zeta) = R(\hat{\mathbf{L}}_B,\zeta)R_{BI}, \tag{8}$$

where $\zeta \equiv \zeta_B + \zeta_I$. This is our parameterization of the attitude matrix in terms of the seven-component state vector

$$\mathbf{x} = \begin{bmatrix} \mathbf{L}_B^T & \mathbf{L}_I^T & \zeta \end{bmatrix}^T. \tag{9}$$

The dynamics are given by (1a), (1b), and a scalar differential equation for ζ.

Reduction to a six-component error state

A straightforward Kalman filter implementation would use the 7×7 covariance $P_x \equiv E\{(\Delta\mathbf{x})(\Delta\mathbf{x})^T\}$ of the error vector $\Delta\mathbf{x} \equiv \mathbf{x} - \bar{\mathbf{x}}$, where $\bar{\mathbf{x}} \equiv E\{\mathbf{x}\}$ is the expectation of $\mathbf{x}$. As pointed out in [2], the constraint of (2) means that this covariance is of rank six, in the same way that the unity norm constraint of the four-component quaternion representation leads to a rank-deficient covariance matrix [3]. In the present case, the covariance matrix must have a null vector $\mathbf{x}_{null}$,

$$P_x\mathbf{x}_{null} = 0_{7\times 1}, \tag{10}$$

that is orthogonal to all the vectors representing physically possible errors in $\mathbf{x}$. The six physically possible errors are a variation in ζ, two independent variations of $\mathbf{L}_B$ perpendicular to $\bar{\mathbf{L}}_B$, two variations of $\mathbf{L}_I$ perpendicular to $\bar{\mathbf{L}}_I$, and simultaneous length-changing equal-magnitude variations of $\mathbf{L}_B$ in the direction of $\bar{\mathbf{L}}_B$ and of $\mathbf{L}_I$ in the direction of $\bar{\mathbf{L}}_I$. Thus the normalized null eigenvector of P_x must be

$$\mathbf{x}_{null} = \pm\frac{1}{\sqrt{2}}\begin{bmatrix} \hat{\bar{\mathbf{L}}}_B^T & -\hat{\bar{\mathbf{L}}}_I^T & 0 \end{bmatrix}^T, \tag{11}$$

which is a vector of errors violating the norm constraint of (2).

We seek a 7×6 matrix S with a Moore-Penrose pseudoinverse [5] S^+ such that

$$S^+S = I_{6\times 6}, \quad SS^+ = I_{7\times 7} - \mathbf{x}_{null}\mathbf{x}_{null}^T, \quad \text{and} \quad S^+\mathbf{x}_{null} = 0_{6\times 1}. \tag{12abc}$$

Note that S and S^+ must be functions of expectations rather than true values, which are unknown by the estimator. The six-dimensional error vector

$$\Delta\mathbf{y} \equiv S^+\Delta\mathbf{x} \tag{13}$$

has a nonsingular 6×6 error covariance P_y given by

$$P_y \equiv E\{(\Delta\mathbf{y})(\Delta\mathbf{y})^T\} = S^+P_x(S^+)^T. \tag{14}$$

Because of (10) and (12b), the 7×7 error covariance P_x can be recovered by

$$SP_yS^T = SS^+P_x(S^+)^TS^T = SS^+P_x(SS^+)^T = P_x \tag{15}$$

and the seven-component error vector, which must be orthogonal to $\mathbf{x}_{null}$, by

$$\Delta\mathbf{x} = I_{7\times7}\Delta\mathbf{x} = (SS^{+} + \mathbf{x}_{null}\mathbf{x}_{null}^{T})\Delta\mathbf{x} = S\Delta\mathbf{y}\,. \tag{16}$$

Having $\Delta\mathbf{L}_B$ as part of $\Delta\mathbf{y}$ would require three rows of S^{+} to be $[I_{3\times3}\ 0_{3\times3}\ 0_{3\times1}]$, and (12c) could not be satisfied. For $\Delta\mathbf{y}$ to contain $\Delta\mathbf{L}_B$, $\hat{\mathbf{L}}_I$ would have to replace of $\mathbf{L}_I$ in $\mathbf{x}$ as in [2]. An analogous situation holds with $\mathbf{L}_I$ and $\mathbf{L}_B$ interchanged.

We choose instead to retain (9) by letting the three attitude error angles in the body reference frame, $\Delta\boldsymbol{\theta}$, be the first three components of $\Delta\mathbf{y}$, for then the upper left-hand corner of P_y is the usual 3×3 attitude error covariance. The expression for $\Delta\boldsymbol{\theta}$ as a function of $\Delta\mathbf{x}$ is found by computing the first-order increment ΔA_{BI} of $A_{BI}(\mathbf{x})$ with variations $\Delta\mathbf{L}_B$, $\Delta\mathbf{L}_I$, and $\Delta\zeta$, and using the relationship

$$[\Delta\boldsymbol{\theta}\times] = -(\Delta A_{BI})A_{BI}^{T}\,. \tag{17}$$

This gives, after considerable algebra,

$$\Delta\boldsymbol{\theta} = -L^{-1}\hat{\mathbf{L}}_B\times[\Delta\mathbf{L}_B - A_{BI}(\mathbf{x})\Delta\mathbf{L}_I] + [\Delta\zeta - L^{-1}\mathbf{w}\cdot(\Delta\mathbf{L}_B + \Delta\mathbf{L}_I)]\hat{\mathbf{L}}_B\,, \tag{18}$$

where

$$\mathbf{w} \equiv (1+\hat{\mathbf{L}}_B\cdot\hat{\mathbf{L}}_I)^{-1}(\hat{\mathbf{L}}_B\times\hat{\mathbf{L}}_I) = (L^2 + \mathbf{L}_B\cdot\mathbf{L}_I)^{-1}(\mathbf{L}_B\times\mathbf{L}_I)\,. \tag{19}$$

Interpreting (18) as a relation of time variations of $\boldsymbol{\theta}$, $\mathbf{L}_B$, $\mathbf{L}_I$, and ζ gives

$$\boldsymbol{\omega}_{BI} = -L^{-1}\hat{\mathbf{L}}_B\times[\dot{\mathbf{L}}_B - A_{BI}(\mathbf{x})\dot{\mathbf{L}}_I] + [\dot{\zeta} - L^{-1}\mathbf{w}\cdot(\dot{\mathbf{L}}_B + \dot{\mathbf{L}}_I)]\hat{\mathbf{L}}_B\,. \tag{20}$$

After substituting (1), (20) reduces to the dynamic equation for ζ,

$$\dot{\zeta} = (1+\hat{\mathbf{L}}_B\cdot\hat{\mathbf{L}}_I)^{-1}[(\hat{\mathbf{L}}_B + \hat{\mathbf{L}}_I)\cdot\boldsymbol{\omega}_{BI} + L^{-1}(\hat{\mathbf{L}}_B\times\hat{\mathbf{L}}_I)\cdot(\mathbf{N}_B + \mathbf{N}_I)]\,. \tag{21}$$

The upper three rows of S^{+} are given by (18). A natural choice for the lower three rows to satisfy (12c) gives

$$S^{+} = \begin{bmatrix} \bar{L}^{-1}\{-[\hat{\bar{\mathbf{L}}}_B\times] - \hat{\bar{\mathbf{L}}}_B\bar{\mathbf{w}}^{T}\} & \bar{L}^{-1}\{[\hat{\bar{\mathbf{L}}}_B\times]A_{BI}(\bar{\mathbf{x}}) - \hat{\bar{\mathbf{L}}}_B\bar{\mathbf{w}}^{T}\} & \hat{\bar{\mathbf{L}}}_B \\ I_{3\times3} & A_{BI}(\bar{\mathbf{x}}) & 0_{3\times1} \end{bmatrix} \tag{22}$$

and

$$\Delta\mathbf{y} = \begin{bmatrix} \Delta\boldsymbol{\theta} \\ \Delta\mathbf{L}_B + A_{BI}(\bar{\mathbf{x}})\Delta\mathbf{L}_I \end{bmatrix}. \tag{23}$$

The pseudoinverse of S^{+} is

$$S = \frac{1}{2}\begin{bmatrix} [\bar{\mathbf{L}}_B\times] & I_{3\times3} \\ -A_{BI}^{T}(\bar{\mathbf{x}})[\bar{\mathbf{L}}_B\times] & A_{BI}^{T}(\bar{\mathbf{x}}) \\ (1+\hat{\bar{\mathbf{L}}}_B\cdot\hat{\bar{\mathbf{L}}}_I)^{-1}[2\hat{\bar{\mathbf{L}}}_B + \hat{\bar{\mathbf{L}}}_I + A_{BI}(\bar{\mathbf{x}})\hat{\bar{\mathbf{L}}}_B]^{T} & \bar{L}^{-1}[\mathbf{w} + A_{BI}(\bar{\mathbf{x}})\mathbf{w}]^{T} \end{bmatrix}. \tag{24}$$

Kalman filter formulation

A Kalman filter for the seven-component state vector $\mathbf{x}$ uses (1) and (21) to propagate the state estimate between observations. The filter update for a measurement $\mathbf{z} = \mathbf{h}(\mathbf{x})$ is given by [6]

$$\mathbf{x}(+) = \mathbf{x}(-) + K_x[\tilde{\mathbf{z}} - \mathbf{h}(-)], \tag{25}$$

where the arguments (–) and (+) denote estimates before and after the update, respectively, $\tilde{\mathbf{z}}$ denotes the measured value, $\mathbf{h}(-) \equiv \mathbf{h}(\mathbf{x}(-))$, and K_x is the Kalman gain. The gain is given by

$$K_x = P_x(-)H_x^T[H_x P_x(-)H_x^T + R]^{-1}, \tag{26}$$

where the measurement sensitivity matrix is

$$H_x \equiv \partial\mathbf{h}(\mathbf{x})/\partial\mathbf{x} \tag{27}$$

and R is the measurement error covariance. The covariance is updated by

$$P_x(+) = (I_{7\times7} - K_x H_x)P_x(-), \tag{28}$$

To avoid using the singular covariance matrix, we substitute (15) into (26), giving

$$K_x = SK_y, \tag{29}$$

where K_y is updated by

$$K_y = P_y(-)H_y^T[H_y P_y(-)H_y^T + R]^{-1} \tag{30}$$

with

$$H_y \equiv H_x S = [\partial\mathbf{h}(\mathbf{x})/\partial\mathbf{x}](\partial\mathbf{x}/\partial\mathbf{y}) = \partial\mathbf{h}/\partial\mathbf{y}. \tag{31}$$

The matrices S and S^+ are always assumed to be evaluated with the pre-update estimates. Substituting (15) into (28) and using (12a) gives

$$P_y(+) = (I_{6\times6} - K_y H_y)P_y(-), \tag{32}$$

The state update is given by

$$\mathbf{x}(+) = \mathbf{x}(-) + SK_y[\tilde{\mathbf{z}} - \mathbf{h}(-)], \tag{33}$$

Defining $\Delta\bar{\boldsymbol{\theta}}$ and $\Delta\bar{\mathbf{y}}_L$ as the first three rows and last three rows of $K_y[\tilde{\mathbf{z}} - \mathbf{h}(-)]$, respectively, we find after some algebra that (24) and (33) give

$$\left|\bar{\mathbf{L}}_I(+)\right|^2 = \left|\bar{\mathbf{L}}_B(+)\right|^2 + \bar{\mathbf{L}}_B(-)\cdot(\Delta\bar{\mathbf{y}}_L \times \Delta\bar{\boldsymbol{\theta}}). \tag{34}$$

The update violates the norm constraint of (2) in second order, in parallel with the quaternion case [3]. Normalizing the updated angular momenta,

$$\hat{\bar{\mathbf{L}}}_B = \bar{\mathbf{L}}_B/\bar{L}_B \quad \text{and} \quad \hat{\bar{\mathbf{L}}}_I = \bar{\mathbf{L}}_I/\bar{L}_I, \tag{35ab}$$

and then redefining the angular momenta by

$$\bar{L} \equiv \sqrt{\tfrac{1}{2}(\bar{L}_B^2 + \bar{L}_I^2)}, \quad \bar{\mathbf{L}}_B = \bar{L}\hat{\bar{\mathbf{L}}}_B, \quad \text{and} \quad \bar{\mathbf{L}}_I = \bar{L}\hat{\bar{\mathbf{L}}}_I. \tag{35cde}$$

restores the constraint while preserving the Euclidean norm of $\bar{\mathbf{x}}$.

The matrices F_y and G_y in the covariance propagation equation

$$\dot{P}_y = F_y P_y + P_y F_y^T + G_y Q G_y^T , \tag{36}$$

are most easily computed directly from the equations for the reduced state vector **y**. To first order in the errors, the attitude error vector obeys the dynamic equation [7]

$$\Delta\dot{\boldsymbol{\theta}} = \Delta\boldsymbol{\omega}_{BI} - \bar{\boldsymbol{\omega}}_{BI} \times \Delta\boldsymbol{\theta} . \tag{37}$$

The angular momentum errors obey the dynamic equation

$$\begin{aligned} \frac{d}{dt}[\Delta\mathbf{L}_B + A_{BI}(\bar{\mathbf{x}})\Delta\mathbf{L}_I] &= \Delta[\mathbf{N}_B - \boldsymbol{\omega}_{BI} \times \mathbf{L}_B] + \dot{A}_{BI}(\bar{\mathbf{x}})\Delta\mathbf{L}_I + A_{BI}(\bar{\mathbf{x}})\Delta[A_{BI}^T(\mathbf{x})\mathbf{N}_B] \\ &= [\bar{\mathbf{L}}_B\times]\Delta\boldsymbol{\omega}_{BI} - [\bar{\boldsymbol{\omega}}_{BI}\times][\Delta\mathbf{L}_B + A_{BI}(\bar{\mathbf{x}})\Delta\mathbf{L}_I] + 2\Delta\mathbf{N}_B - [\mathbf{N}_B\times]\Delta\boldsymbol{\theta} , \end{aligned} \tag{38}$$

using $A_{BI}^T(\mathbf{x}) \approx A_{BI}^T(\bar{\mathbf{x}})(I_{3\times3} + [\Delta\boldsymbol{\theta}\times])$. From (3), (16), (23), and (24) we have

$$\Delta\boldsymbol{\omega}_{BI} = \tfrac{1}{2} J^{-1}\{[\bar{\mathbf{L}}_B\times]\Delta\boldsymbol{\theta} + [\Delta\mathbf{L}_B + A_{BI}(\bar{\mathbf{x}})\Delta\mathbf{L}_I]\} - J^{-1}\Delta\mathbf{L}_{int} . \tag{39}$$

Then

$$\Delta\dot{\mathbf{y}} = F_y\Delta\mathbf{y} + G_y\begin{bmatrix} -J^{-1}\Delta\mathbf{L}_{int} \\ \Delta\mathbf{N}_B \end{bmatrix}, \tag{40a}$$

with

$$F_y \equiv \begin{bmatrix} \tfrac{1}{2}J^{-1}[\bar{\mathbf{L}}_B\times] - [\bar{\boldsymbol{\omega}}_{BI}\times] & \tfrac{1}{2}J^{-1} \\ \tfrac{1}{2}[\bar{\mathbf{L}}_B\times]J^{-1}[\bar{\mathbf{L}}_B\times] - [\mathbf{N}_B\times] & \tfrac{1}{2}[\bar{\mathbf{L}}_B\times]J^{-1} - [\bar{\boldsymbol{\omega}}_{BI}\times] \end{bmatrix}, \tag{40b}$$

and

$$G_y \equiv \begin{bmatrix} I_{3\times3} & 0_{3\times3} \\ [\bar{\mathbf{L}}_B\times] & 2I_{3\times3} \end{bmatrix}. \tag{40c}$$

These and

$$Q = \begin{bmatrix} Q_{int} & 0_{3\times3} \\ 0_{3\times3} & Q_{ext} \end{bmatrix} \tag{41a}$$

with

$$Q_{int}\,\delta(t-t') = J^{-1}E\{\Delta\mathbf{L}_{int}(t)\Delta\mathbf{L}_{int}^T(t')\}J^{-1} \tag{41b}$$

and

$$Q_{ext}\delta(t-t') = E\{\Delta\mathbf{N}_B(t)\Delta\mathbf{N}_B^T(t')\} \tag{41c}$$

are the matrices needed for the covariance propagation. Note that Q_{int} may be non-zero even for a nominally rigid spacecraft.

Neither S^+ nor the singular covariance P_x appears in our Kalman filter, which uses (30), (32), (33), and (36); and S only appears in (33). It may be desirable to compute P_x to exhibit the covariance of $\mathbf{L}_I$ and $\mathbf{L}_B$, however.

Filter implementation

The spinning spacecraft EKF has been implemented in MATLAB as a subsystem of the Multimission Spin-Axis Stabilized Spacecraft Attitude Ground Support System that has supported NASA Goddard Space Flight Center missions for many years. The new EKF subsystem adds the capability to solve for a time-dependent attitude history and could be used for real-time applications, if needed. The software comprises a driver, an EKF main routine, and subroutines for time propagation, measurement sensitivity matrix computation, and filter updates. The driver processes sensor data and presents it to the filter as vector observations. After discarding bad data points, the EKF main routine calls the propagation subroutine to integrate the state vector and its covariance to the next observation time, using a 4^{th}-order Runge-Kutta integrator with an appropriate time step. The EKF main routine obtains the spacecraft ephemeris and geomagnetic field and computes torques due to gravity gradients and any residual constant spacecraft magnetization at each integration step [4]. Then the sensor residual and the sensitivity matrix are computed, and the state and covariance are updated.

Singularity avoidance

It is clear throughout the development of this filter that the spacecraft angular momentum must be nonzero, but it is easily seen that the algorithm is also singular when $\mathbf{L}_B$ and $\mathbf{L}_I$ are 180° apart. The software checks for this singular condition and redefines the inertial reference frame so that $\mathbf{L}_I$ is always greater than a user-specified distance from $-\mathbf{L}_B$ in the modified frame, transforming all reference vectors along with $\mathbf{L}_I$. Reconstructing the usual attitude is only a matter of keeping track of these reference frame rotations, which are all handled internally and are totally transparent to the user of the software.

Vector measurement model

It is easier to calculate the sensitivity matrix for a vector measurement directly from the six-component $\mathbf{y}$ than from the seven-component $\mathbf{x}$. For this model, $\mathbf{z} = \mathbf{v}_B$ and

$$\mathbf{h}(\mathbf{x}) = A_{BI}(\mathbf{x})\mathbf{v}_I \simeq (I_{3\times3} - [\Delta\boldsymbol{\theta}\times])A_{BI}(\bar{\mathbf{x}})\mathbf{v}_I = \bar{\mathbf{v}}_B + \bar{\mathbf{v}}_B \times \Delta\boldsymbol{\theta} \ , \tag{42}$$

where

$$\bar{\mathbf{v}}_B \equiv A_{BI}(\bar{\mathbf{x}})\mathbf{v}_I \ . \tag{43}$$

It follows from (23) and the rightmost part of (31) that

$$H_y = \left[[\bar{\mathbf{v}}_B\times] \quad 0_{3\times3} \right]. \tag{44}$$

Testing

Several tests were performed to compare results from the filter described in this paper, the filter presented in [2], and the Unit Vector Filter (UVF) [9] that has supported many three-axis stabilized spacecraft at Goddard Space Flight Center over the past 12 years. For application to spinning spacecraft, the UVF has been modified to estimate the quaternion and rotation rate rather than the gyro biases, to

use dynamics propagation rather than gyro propagation, and to include a J-dependent term in the linearized dynamics matrix used for covariance propagation:

$$F_{UVF} = \begin{bmatrix} -[\boldsymbol{\omega}\times] & -I \\ 0_{3\times 3} & J^{-1}\left([J\boldsymbol{\omega}\times]-[\boldsymbol{\omega}\times]J\right) \end{bmatrix}. \tag{45}$$

Simulation parameters

The tests exercised all the key features of the filter using simulated data based on parameters from the ST5 series of spinning spacecraft [8]. These are small (25 kg) spacecraft in highly eccentric orbits with apogee and perigee altitudes of 4500 km and 300 km, respectively, period of about 136 minutes, and inclination 105.6°. The spacecraft spin at 26 revolutions per minute (rpm), nominally about the z axis. The sensor complement is a three-axis magnetometer (TAM) and a slit Sun sensor that detects a Sun pulse and the Sun elevation angle from the nominal spin plane once per spin. The Sun elevation measurement and known slit azimuth angle are combined into an observed Sun unit vector for the EKF. The EKF processes 8 TAM measurements per second, the rate at which they are telemetered to the ground. The moment of inertia tensor for the fully deployed configuration of ST5 has been simplified to be axially symmetric,

$$J_{true} = diag([0.8, 0.8, 1.12])\ \mathrm{kg\,m^2}. \tag{46}$$

A single cold gas microthruster is used to perform attitude and trajectory maneuvers. The environmental torque models were turned off for the simulation.

Six tests were performed, each 20 minutes in length and ending about 3 minutes before the spacecraft passes perigee. The initial attitude and rate errors were 45° and 1.0 deg/sec on the z (spin) axis and 10° and 0.1 deg/sec on the transverse axes in all the tests. The sensor noise in both the truth model and for EKF tuning are Gaussian with standard deviations of 0.1° for the Sun elevation, 0.0007 sec for the Sun pulse time, and 0.2 μT per axis for the TAM. The process noise is taken to be

$$Q_{int} = 10^{-6}\,\mathrm{rad^2/sec} \times diag([1, 1, 3]) \tag{47a}$$

and

$$Q_{ext} = 0.1\,\mathrm{sec^{-2}} \times J_{EKF} Q_{int} J_{EKF}, \tag{47b}$$

where J_{EKF} is the inertia tensor modeled by the EKF. This is equal to the true inertia tensor for the first four simulations. The details of the tests are described briefly below, and the results are summarized in Table 1.

Tests 1–3: Torque-free rotation with nutation

The first three tests simulate simple torque-free motion with nutation angle of 0, 2°, and 4°, respectively. Figure 1 shows the attitude errors relative to the truth model for the 4° nutation test. It can be seen that the new filter performs quite well, and that the combination of Sun sensor and magnetometer data will provide excellent attitude determination performance for ST5.

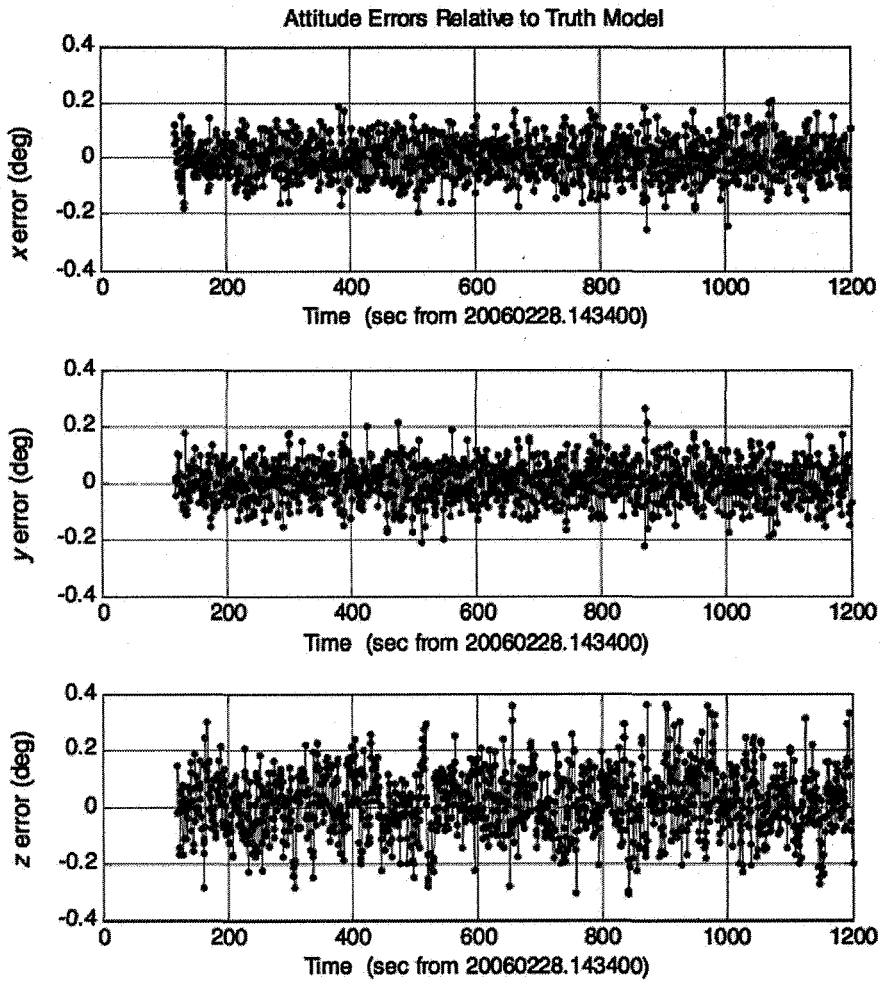

Figure 1: Attitude errors for 4° nutation, perfect inertia modelling, and no slew.

Test 4*: *Attitude reorientation

This tests the ability of the filter to follow a large 360° attitude reorientation slew over a 20 minute time span. The slew was simulated with zero nutation. The results in Table 1 show that the slew is tracked very well, with attitude estimates equally accurate as those for the maneuver-free tests.

Tests 5 & 6: Inertia tensor mismatch

These test the ability of the filter to deal with a mismatch between the true inertia tensor and the filter's knowledge of it. The EKF in Tests 1–4 used the true inertia tensor of (46). For tests 5 and 6, the filter used an inertia tensor close to the actual value predicted for the ST5 spacecraft

$$J_{EKF} = \begin{bmatrix} 0.630 & -0.100 & 0.005 \\ -0.100 & 0.950 & 0.007 \\ 0.005 & 0.007 & 1.220 \end{bmatrix} \text{kg m}^2 . \qquad (48)$$

Other than this, Tests 5 and 6 are the same as Tests 3 and 4, respectively. Figure 2 shows the attitude errors relative to the truth model for Test 5, with 4° nutation and no maneuver. Comparison of this figure with Figure 1 clearly shows the importance of accurate inertia modelling for spinning spacecraft.

Table 1 summarizes the results of the six tests. The last three columns give the root-mean-square attitude errors for the three algorithms: the new algorithm presented in this paper, the closely related algorithm of [2], and the Unit Vector Filter. The statistics were collected over the last 18 minutes of each test, with the first two minutes omitted to eliminate the effects of initialization transients. The pointing errors are slightly smaller for the new filter, but the difference is barely significant except for the tests with mismodelled inertia. The new filter appears to be more tolerant of inertia mismodelling than the other filters. The differences may very well be due to differences in the process noise tuning, though, rather than to the fundamental superiority of the new algorithm. Each 20-minute simulation required about 25 sec for the new filter, 35 sec for the filter of [2], and 18 sec for the UVF. The absolute times are platform-dependent, but the relative times are significant.

Test number and description		RMS error (deg)		
		New	[2]	UVF
1	No maneuver, perfect inertia, 0 nutation	0.146	0.169	0.168
2	No maneuver, perfect inertia, 2° nutation	0.148	0.163	0.162
3	No maneuver, perfect inertia, 4° nutation	0.148	0.160	0.159
4	360° slew, perfect inertia, 0 nutation	0.147	0.161	0.157
5	No maneuver, mismodelled inertia, 4° nutation	3.07	5.21	5.16
6	360° slew, mismodelled inertia, 0 nutation	2.31	4.05	3.88

Table 1. Attitude errors for the six tests of the three filtering algorithms.

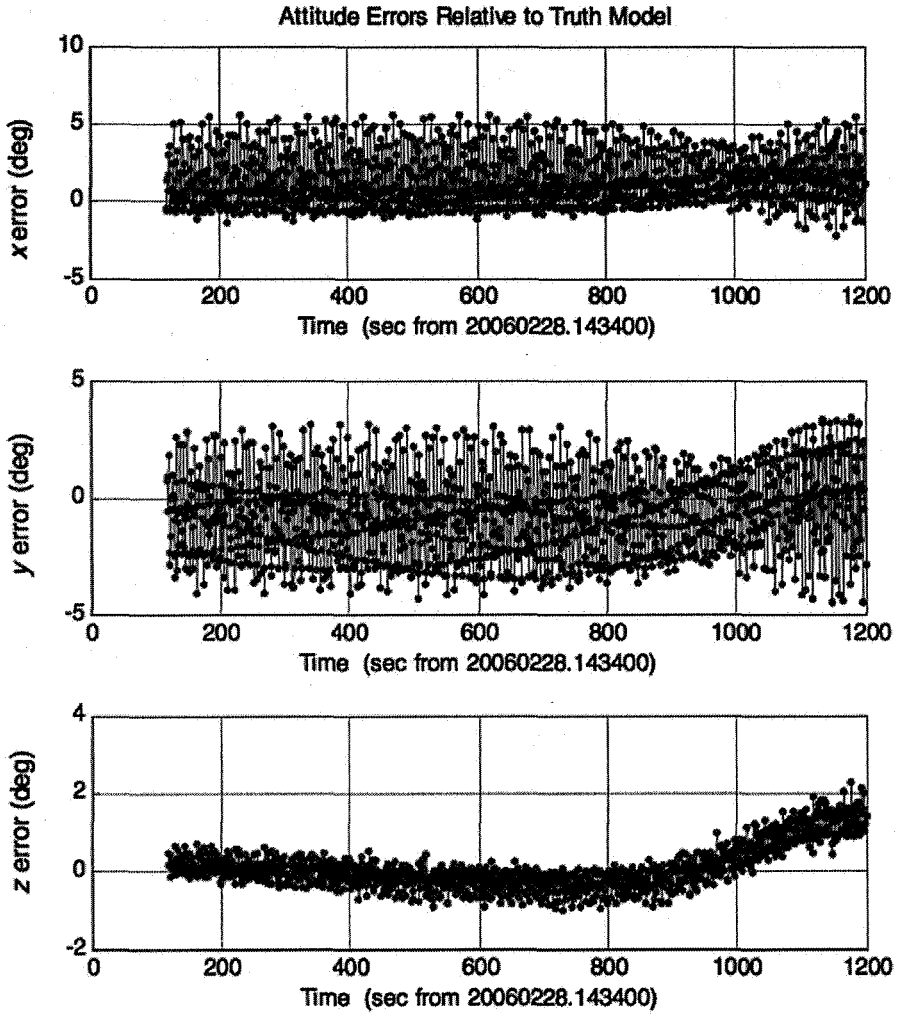

Figure 2. Attitude errors for 4° nutation, mismodelled inertia, and no slew.

Conclusions

The new spinning spacecraft EKF has been shown to perform well under several test scenarios. Its initial convergence is very robust, and its attitude accuracy is about 10% better than either a conventional quaternion-based filter or an earlier filter implementation using momentum-based attitude parameters. This improved performance may result from a superior expression for process noise, facilitating filter tuning, or from improved covariance propagation. Additional development and testing will search for further improvements in the new filter. Regardless, this work has succeeded in providing two powerful filters for attitude determination of spinning spacecraft, adding a significant new capability to the attitude ground support system at the NASA Goddard Space Flight Center.

Ongoing work is investigating how to determine sensor biases, scale factors, misalignments, and time-tag errors, either along with the attitude state or in a parallel utility. Several types of biases are already estimated as part of the current batch-method spinning spacecraft attitude ground support system, where the spin vector is assumed to be constant for the entire batch. However, it may be useful for early mission support to be able to determine the biases before the nutation has fully damped out and the motion is a simple principal axis spin.

References

[1] Markley, F. L., New Dynamic Variables for Momentum-Bias Spacecraft, *Journal of the Astronautical Sciences*, Vol. 41, No. 4 (557–567), 1993.

[2] Sedlak, J. E., Spinning Spacecraft Attitude Estimation Using Markley Variables: Filter Implementation and Results, 2005 Flight Mechanics Symposium, Goddard Space Flight Center, Greenbelt, MD, NASA Conference Publication NASA/CP-2005-212789, October 2005.

[3] Lefferts, E. J., Markley, F. L., and Shuster, M. D., Kalman Filtering for Spacecraft Attitude Estimation, *Journal of Guidance, Control, and Dynamics*, Vol. 5, No. 5 (417–429), 1982.

[4] Wertz, J. R., ed., *Spacecraft Attitude Determination and Control*, D. Reidel, Dordrecht, Holland, Chapter 16, 1978.

[5] Golub, Gene H. and Charles F. Van Loan, *Matrix Computations*, Baltimore, MD, The Johns Hopkins University Press (139),1983.

[6] Gelb, Arthur, ed., *Applied Optimal Estimation*, Cambridge, MA, the MIT Press, 1974.

[7] Shuster, Malcolm D., A Survey of Attitude Representations, *Journal of the Astronautical Sciences*, Vol. 41, No. 4 (439–517), 1993.

[8] D. Speer, G. Jackson, K. Stewart, and A. Hernandez-Pellerano, *The Space Technology 5 Avionics System System*, 2005 IEEE Aerospace Conference, Big Sky, MT, 05–12 March 2005.

[9] J. Sedlak and D. Chu, "Kalman Filter Estimation of Attitude and Gyro Bias with the QUEST Observation Model," AAS 93-297, *Proceedings of the AAS/GSFC International Symposium on Space Flight Dynamics*, Greenbelt, MD, 1993.